EFFECTIVE ACCEPTANCE EVALUATION OF LINEAR RESONANCE ACCELERATOR

V.S. Dyubkov, É.S. Masunov
Chair of Electrophysical Facilities, National Research Nuclear University (MEPhI), Moscow, Russia
E-mail: vsdyubkov@mephi.ru

One of the most important challenges for accelerators is to match an accelerating beam with an accelerator acceptance. It allows one reduce a particle loss. Effective acceptance evaluation of linear resonance accelerator with RF focusing is carried out with no taking into account a beam space charge; a model taking into account non-coherent bunch particle oscillations is considered with the use of an averaging technique over rapid oscillations. Analytical results obtained are verified. Computer simulations of self-consistent low-energy ion beam dynamics are performed.

PACS: 02.30.Em; 41.75.Lx

1. INTRODUCTION

One of the most urgent problems of accelerator engineering to date is a design and development of high-performance high-current systems for an injection and acceleration of low-velocity heavy-ion beams. This problem as well as others cannot be solved without taking into account problem solution on beam emittance matching with an acceptance of an accelerator channel. Effective acceptance evaluation for the resonance accelerator channel depends on a mathematical model used for describing a beam dynamics. Effective acceptance evaluation of the resonance accelerator channel was performed previously on basis of charged particle beam oscillation as a whole [1-4], that is under the assumption of coherent oscillations of individual particles. It is evident that this model does not correspond to real conditions in the beam given completely but it allows one make some important estimation. It is of particular interest to consider a model, which is taking into account non-coherent particle oscillations in the beam, and analyze results based on it.

2. ACCEPTANCE EVALUATION

It is difficult to analyze a beam dynamics in a high frequency polyharmonic field. Therefore, we will use one of methods of an averaging over a rapid oscillations period, following the formalism presented in Ref. [1–4]. The first to use an averaging method was P.L. Kapitsa [5]. One first expresses RF field in an axisymmetric periodic resonant structure as Fourier's representation by spatial harmonics of a standing wave assuming that the structure period is a slowly varying function of a longitudinal coordinate z

$$E_{\|} = \sum_{n=0}^{\infty} E_n I_0(k_n r)\cos\left(\int k_n dz\right)\cos\omega t;$$
$$E_{\perp} = \sum_{n=0}^{\infty} E_n I_1(k_n r)\sin\left(\int k_n dz\right)\cos\omega t, \tag{1}$$

where E_n is the nth harmonic amplitude of RF field on the axis; $k_n = (\theta + 2\pi n)/D$ is the propagation wave number for the nth RF field spatial harmonic; D is the resonant structure geometric period; θ is the phase advance per D period; ω is the circular frequency; I_0, I_1 are modified Bessel functions of the first kind.

As it was stated above, we will take into account non-coherent particle oscillations in the beam being accelerated. To this end, one introduces a notion of a reference particle, i.e. a particle moving on the channel axis. This particle is at the point with coordinates (z_r; 0) at given moment of time (subscript "r" means a value for the reference particle). A magnetic force can be neglected for low-energy ions. We will assume that $dz/dr << 1$. Then, one passes into the reference particle rest frame. There is a differentiation over longitudinal coordinate in the beam motion equation. Thus, the motion equation together with an equation of particle phase variation can be presented in a view of a system of the first order differential equations as follows

$$\begin{cases} \dfrac{d\Theta}{d\xi} = e_{\|}(z,0,t_r) - e_{\|}(z,0,t); \\ \dfrac{d\beta_{\perp}}{d\xi} = \dfrac{e_{\perp}(z,r,t)}{\beta_{\|}}; \\ \dfrac{d\psi}{d\xi} = \dfrac{1}{\beta_{\|}} - \dfrac{1}{\beta_{\|r}}. \end{cases} \tag{2}$$

Here we introduced the following dimensionless variables: $\Theta = \gamma_r - \gamma$, γ is the Lorentz's factor; $\xi = 2\pi z/\lambda$, $e_{\|,\perp} = eE_{\|,\perp}Z\lambda/2\pi m_0 c^2$, e is the elementary charge, Z is a charge state of an ion, λ is a wave length of RF field, m_0 is an ion rest mass, c is the light velocity in free space; $\beta_{\|,\perp} = \upsilon_{\|,\perp}/c$, $\psi = \omega(t - t_r)$. Note, it can be assumed that $\Theta \approx \beta_s(\beta_{\|r} - \beta_{\|})$, where β_s is the equilibrium particle velocity and s is a number of the synchronous harmonic, provided $|\beta_{\|} - \beta_s| << 1$ is satisfied. Therefore, we can write $d\psi/d\xi \approx (\beta_{\|r} - \beta_{\|})/\beta_s^2$ for the last equation of the system (2). Now the first and the third equations of the system (2) can be united as follows

$$\frac{d^2\psi}{d\xi^2} + 3\kappa(\xi)\frac{d\psi}{d\xi} = \frac{1}{\beta_s^3}\frac{d\Theta}{d\xi}, \tag{3}$$

and the second equation of the system (2) can be rewritten in the form

$$\frac{d^2\delta}{d\xi^2} + \kappa(\xi)\frac{d\delta}{d\xi} = \frac{e_{\perp}}{\beta_s^3}, \tag{4}$$

where $\delta = 2\pi r/\beta_s\lambda$ is the dimensionless transverse variable and $\kappa = (\ln\beta_s)'_{\xi}$. On averaging over rapid oscillation period one can present the motion equation in the smooth approximation with the restrictions mentioned above in the following matrix form

$$\ddot{Y} + \Lambda\dot{Y} = -LU_{\text{ef}}, \tag{5}$$

where the dot above stands for differentiation with respect to the independent ξ variable. Hereafter ψ and δ mean its averaged values and

$$Y = \begin{pmatrix}\psi\\ \delta\end{pmatrix}, \quad \Lambda = \begin{pmatrix}3\kappa & 0\\ 0 & \kappa\end{pmatrix}, \quad L = \begin{pmatrix}\frac{\partial}{\partial\psi}\\ \frac{\partial}{\partial\delta}\end{pmatrix}. \tag{6}$$

U_{ef} is an effective potential function (EPF) describing a two-dimensional low-energy beam interaction with the polyharmonical field of the system subject to the incoherent particle oscillations. EPF allows the beam dynamics to be investigated carefully. For the Wideröe type structure EPF can be expressed as

$$U_{\text{ef}} = \sum_{i=0}^{4} U_i; \tag{7}$$

$$\begin{aligned}
U_0 &= \frac{e_s}{2\beta_s}\left[I_0(\delta)\sin(\psi+\phi_r) - \psi\cos\phi_r - \sin\phi_r\right];\\
U_1 &= \frac{1}{16}\sum_{n\neq s}^{\infty}\frac{e_n^2}{\nu_{s,n}^2}w_{n,s}^{(0)}(\delta) + \frac{1}{16}\sum_{n=0}^{\infty}\frac{e_n^2}{\mu_{s,n}^2}w_{n,s}^{(0)}(\delta);\\
U_2 &= -\frac{1}{8}\sum_{n\neq s}^{\infty}\frac{e_n^2}{\nu_{s,n}^2}\left[I_0(\iota_{n,s}\delta)\cos\psi - 1\right] - \frac{1}{8}\sum_{n=0}^{\infty}\frac{e_n^2}{\mu_{s,n}^2}\left[I_0(\iota_{n,s}\delta)\cos\psi - 1\right];\\
U_3 &= -\frac{1}{8}\sum_{\substack{n\neq s\\ k_n-k_p=2k_s}}^{\infty}\frac{e_ne_p}{\nu_{s,n}^2}\left\{\left[I_0(\iota_{n,s}\delta) + I_0(\iota_{p,s}\delta)\right]\cos(\psi+2\phi_r) - 2\cos 2\phi_r\right\} - \frac{1}{8}\sum_{\substack{n\neq s\\ k_n+k_p=2k_s}}^{\infty}\frac{e_ne_p}{\nu_{s,n}^2}\left[I_0(\iota_{n,s}\delta)\cos(\psi+2\phi_r) - \cos 2\phi_r\right];\\
U_4 &= \frac{1}{8}\sum_{\substack{n\neq s\\ k_n-k_p=2k_s}}^{\infty}\frac{e_ne_p}{\nu_{s,n}^2}\left[w_{n,s,p}^{(1)}(\delta)\cos(2\psi+2\phi_r) - \cos 2\phi_r\right] + \frac{1}{16}\sum_{\substack{n\neq s\\ k_n+k_p=2k_s}}^{\infty}\frac{e_ne_p}{\nu_{s,n}^2}\left[w_{n,s,p}^{(2)}(\delta)\cos(2\psi+2\phi_r) - \cos 2\phi_r\right].
\end{aligned} \tag{8}$$

Here $e_n = eE_nZ\lambda/2\pi\beta_s^2m_0c^2$; ϕ_r is the reference particle phase; $\nu_{s,n} = (k_s - k_n)/k_s$, $\mu_{s,n} = (k_s + k_n)/k_s$, $\iota_{n,s} = k_n/k_s$, $s, n, p = 0, 1, 2, \ldots$ and the functions of the dimensionless transverse coordinate are defined as

$$\begin{aligned}
w_{n,s}^{(0)} &= I_0^2(\iota_{n,s}\delta) + I_1^2(\iota_{n,s}\delta) - 1;\\
w_{n,s,p}^{(1)} &= I_0(\iota_{n,s}\delta)I_0(\iota_{p,s}\delta) + I_1(\iota_{n,s}\delta)I_1(\iota_{p,s}\delta);\\
w_{n,s,p}^{(2)} &= I_0(\iota_{n,s}\delta)I_0(\iota_{p,s}\delta) - I_1(\iota_{n,s}\delta)I_1(\iota_{p,s}\delta).
\end{aligned} \tag{9}$$

From these expressions, we can see that the term U_0 of EPF is responsible for both the beam acceleration and its transverse defocusing. The term U_1 influences only the transverse motion, always focusing the beam in the transverse direction. The terms U_2, U_3, U_4 have an influence not only on the longitudinal motion but also on the transverse one.

To define eigenfrequencies of small system vibrations, EPF is expanded in Maclaurin's series

$$U_{\text{ef}} = \frac{\Omega_{0\psi}^2\psi^2}{2} + \frac{\Omega_{0\delta}^2\delta^2}{2} + o\left(Y^{\mathrm{T}}Y\right), \tag{10}$$

and the coefficients in which are given by

$$\begin{aligned}
\Omega_{0\psi}^2 &= -\frac{e_s}{2\beta_s}\sin\phi_r + \frac{1}{8}\sum_{n\neq s}^{\infty}\frac{e_n^2}{\nu_{s,n}^2} + \frac{1}{8}\sum_{n=0}^{\infty}\frac{e_n^2}{\mu_{s,n}^2} - \frac{1}{4}\sum_{\substack{n\neq s\\ k_n-k_p=2k_s}}^{\infty}\frac{e_ne_p}{\nu_{s,n}^2}\cos 2\phi_r - \frac{1}{8}\sum_{\substack{n\neq s\\ k_n+k_p=2k_s}}^{\infty}\frac{e_ne_p}{\nu_{s,n}^2}\cos 2\phi_r;\\
\Omega_{0\delta}^2 &= \frac{e_s}{4\beta_s}\sin\phi_r + \frac{1}{32}\sum_{n\neq s}^{\infty}\frac{\iota_{n,s}^2}{\nu_{s,n}^2}e_n^2 + \frac{1}{32}\sum_{n=0}^{\infty}\frac{\iota_{n,s}^2}{\mu_{s,n}^2}e_n^2 + \frac{1}{16}\sum_{\substack{n\neq s\\ k_n-k_p=2k_s}}^{\infty}\frac{\iota_{n,s}\iota_{p,s}}{\nu_{s,n}^2}e_ne_p\cos 2\phi_r + \frac{1}{32}\sum_{\substack{n\neq s\\ k_n+k_p=2k_s}}^{\infty}\frac{\iota_{p,s}^2 - \iota_{n,s}^2 - \iota_{n,s}\iota_{p,s}}{\nu_{s,n}^2}e_ne_p\cos 2\phi_r.
\end{aligned} \tag{11}$$

A character of the vibrations will depend on ratio between the dissipative coefficient κ and eigenfrequencies. It is necessary that $\Omega_{0\psi}^2 > 0$, $\Omega_{0\delta}^2 > 0$ for the vibration process.

Changing the total mechanical energy E, that is $E = 0.5\dot{Y}^{\mathrm{T}}\dot{Y} + U_{\text{ef}}$, is defined by the following equation

$$\frac{dE}{d\xi} = -2\Phi, \tag{12}$$

where $\Phi = 0.5\dot{Y}^{\mathrm{T}}\Lambda\dot{Y}$ is Rayleigh-Onsager function.

A capture region allows for the fact of an explicit dependence of system Hamiltonian on ξ variable is calculated numerically.

3. COMPUTER SIMULATION RESULTS

The analytical results obtained above were used to investigate the beam matching possibility at the linac output. The beam was the unbunched 2.5 keV/u lead ions Pb^{25+} with charge-to-mass ratio is equal to 0.12. We consider there are two spatial harmonics at the linac. One of it is the synchronous harmonic with $s = 0$, and another one is the nonsynchronous (focusing) with $n = 1$. Self-consistent beam dynamics simulations were conducted by means of a modified version of the specialized computer code BEAMDULAC–ARF3 based on CIC technique to calculate beam self-space-charge field. At the beginning, computer simulations were made for the linac structure under the following parameters: $\lambda = 8.88$ m; system length $L = 2.44$ m; bunching length (L_b) and field increasing one (L_f) are the same and the former being equal to 1.75 m; channel aperture $a = 5$ mm; input/output value of the equilibrium particle phase $\varphi_s = -0.5\pi/-0.125\pi$; synchronous harmonic maximal value at the axis is equal to 42.67 kV/cm; ratio of the harmonic amplitudes $\chi = e_1/e_0$ is equal to 4. The equilibrium particle phase linearly increases at the bunching length and plateaus further. Note that the variation of the synchronous harmonic amplitude against longitudinal coordinate (at the length L_f) was calculated by using the technique described in [1]. Initial beam radius and current were 1 mm and 5 μA respectively. The output beam energy and current transmission coefficient were 260 keV/u and 85% in this case. 4D beam phase volume projections onto $(\psi, \dot{\psi})$ phase plane together with phase paths at linac input and output are shown in Fig.1 and Fig.2 correspondingly. The projections of the beam phase volume onto $(\delta, \dot{\delta})$ phase plane together with RMS emittances are shown in Fig.3. Eigenfrequencies variations along the linac as well as dissipative coefficient are shown in Fig.4. Fig.2 illustrates rather fine beam bunching at the output, but Fig.4 shows that $\Omega_{0\delta}^2 \le 0$ all along. Due to this fact, the output beam radius is nearly 5 times as high as the input one.

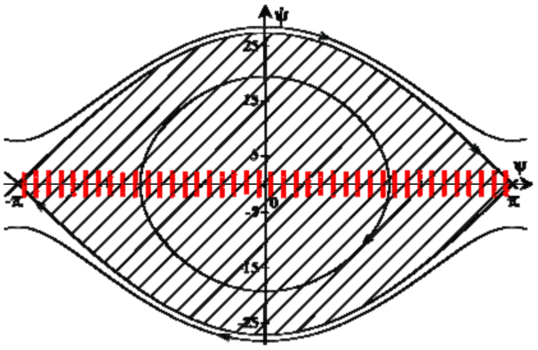

Fig.1. Initial beam distribution in the $(\psi,\dot{\psi})$ plane

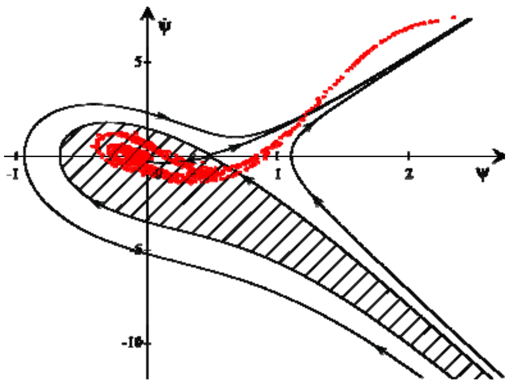

Fig.2. Resulting beam distribution in the $(\psi,\dot{\psi})$ plane

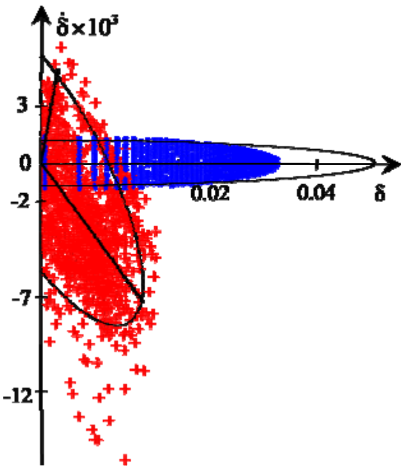

Fig.3. 4D beam phase volume projection onto $(\delta,\dot{\delta})$: "•" and "+" correspond to the input and output one

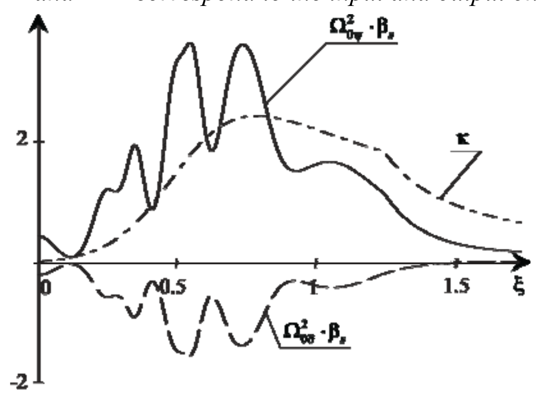

Fig.4. Normalized eigenfrequencies and dissipative coefficient versus longitudinal coordinate

It is worth pointing out that the parameters presented were chosen to ensure the necessary output energy and the beam matching question was not taken into account.

To fulfill beam matching at the linac output, i.e. output beam radius should be equal to input one or so, we decided to reduce acceleration rate so as to guarantee a positivity of the eigenfrequency of the small transverse tunes at least near the output.

Thus, the all previous parameters were kept the same except for the following ones: the synchronous harmonic maximal value at the axis was changed to 16.08 kV/cm, output value of the equilibrium particle phase to $-\pi/6$ and the ratio of the harmonic amplitudes to 9. Under this conditions the output beam energy and current transmission coefficient are 103 keV/u and 85% respectively. The particle loss is observed in longitudinal direction in both cases.

4D beam phase volume projections onto $(\psi,\dot{\psi})$ phase plane together with phase paths calculated in keeping with Eq. (5) at linac input and output are shown in Fig.5 and Fig.6 for this case.

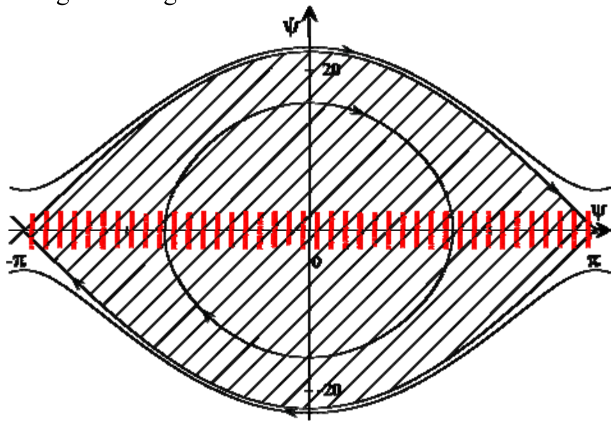

Fig.5. Initial beam distribution in the $(\psi,\dot{\psi})$ plane

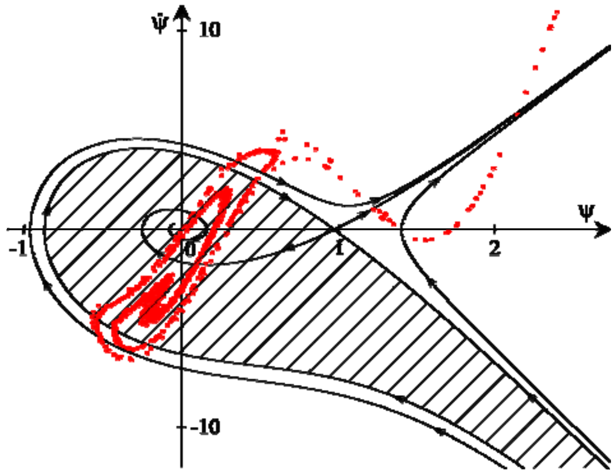

Fig.6. 4D beam phase volume projection onto $(\psi,\dot{\psi})$ phase plane and phase paths

The projections of the beam phase volume onto $(\delta,\dot{\delta})$ phase plane together with RMS emittances are shown in Fig.7. Variations of the eigenfrequencies and dissipative coefficient throughout the linac are shown in Fig.8. Fig.8 shows that $\Omega_{0\psi}^2 > 0$ and $\Omega_{0\delta}^2 > 0$ starting from $\xi = 0.9$. The output beam radius is nearly 1.5 times greater than the input one because of this fact. This result is acceptable.

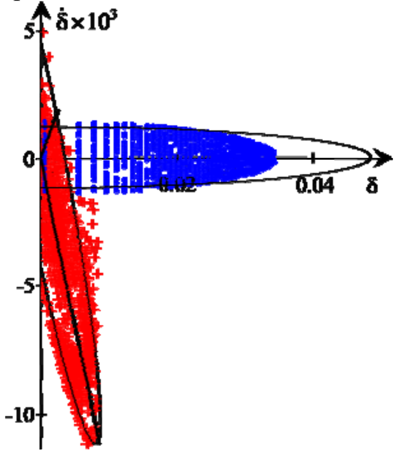

Fig.7. 4D beam phase volume projection onto $(\delta,\dot{\delta})$: "•" and "+" correspond to the input and output one

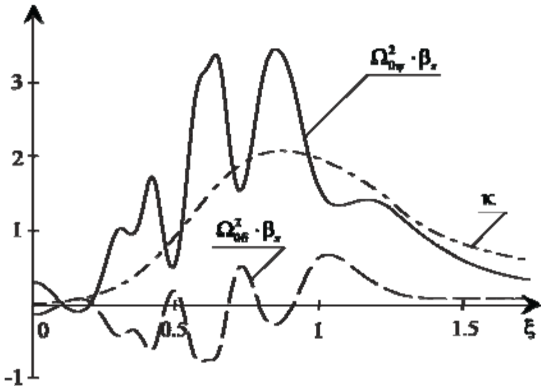

Fig.8. Reduced eigenfrequencies and dissipative coefficient vs longitudinal coordinate

It is worth-while to compare phase capture regions on $\psi = 0$ level at the linac output for conservative and nonconservative approximations in both cases. For the former one, capture region in nonconservative approximation is about 38% more than that for conservative approximation. For the latter, capture region in nonconservative approximation is about 21% more as compared with conservative one.

SUMMARY

Beam dynamics model with regard for particles noncoherent oscillations was made. Effective acceptance evaluation in terms of this model was evaluated. The necessary restrictions on the linac parameters were imposed to make beam matching at the output. The numerical simulations of the self-consistent low-velocity heavy-ion beam dynamics confirmed the analytical results obtained.

ACKNOWLEDGEMENTS

On behalf of friends and colleagues, author pays respect to Prof. Eduard Sergeevich Masunov's family in connection with his sudden decease.

REFERENCES

1. V.S. Dyubkov, E.S. Masunov. Investigation and optimization of low-energy heavy-ion beam dynamics in periodic axisymmetrical structures with dc focusing // *International Journal of Modern Physics A*. 2009, v.24, №5, p.843-856.
2. E.S. Masunov, N.E. Vinogradov. RF focusing of ion beams in the axisymmetric periodic structure of a linear accelerator // *Zhurnal Tekhnicheskoi Fiziki*. 2001, v.71, №9, p.79-87 (in Russian).
3. E.S. Masunov, S.M. Polozov. Ion beam acceleration and focusing in RF structures with undulators // *Zhurnal Tekhnicheskoi Fiziki*. 2005, v.75, №7, p.112-118 (in Russian).
4. E.S. Masunov, V.S. Dyubkov. Comparison of two focusing methods in low-energy ion linac with electric undulator fields // *Problems of Atomic Science and Technology. Series "Nuclear Physics Investigations" (49)*. 2008, №3, p.166-170.
5. P.L. Kapitsa. Dynamic stability of a pendulum with an oscillating suspension point // *Zhurnal Eksperimental'noi i Teoreticheskoi Fiziki*. 1951, v.21, №.5, p.588-597 (in Russian).

Статья поступила в редакцию 07.09.2009 г.

ОЦЕНКА ЭФФЕКТИВНОГО АКСЕПТАНСА ЛИНЕЙНОГО РЕЗОНАНСНОГО УСКОРИТЕЛЯ

В.С. Дюбков, Э.С. Масунов

Одной из наиболее важных задач для ускорителей является задача согласования ускоряемого пучка с аксептансом ускорителя, решение которой позволяет снизить потери частиц пучка. Производится оценка эффективного аксептанса (области захвата) линейного резонансного ускорителя с ВЧ-фокусировкой без учёта поля собственного пространственного заряда пучка; рассматривается модель, учитывающая некогерентные колебания частиц сгустка, с использованием метода усреднения по быстрым осцилляциям. Полученные аналитические результаты проверяются. Проводятся численные моделирования самосогласованной динамики низкоэнергетического ионного пучка.

ОЦІНКА ЕФЕКТИВНОГО АКСЕПТАНСУ ЛІНІЙНОГО РЕЗОНАНСНОГО ПРИСКОРЮВАЧА

В.С. Дюбков, Е.С. Масунов

Одним із найбільш важливих завдань для прискорювачів є завдання узгодження прискорюючого пучка з аксептансом прискорювача, рішення якого дозволяє знизити втрати частинок пучка. Проводиться оцінка ефективного аксептанса (області захоплення) резонансного лінійного прискорювача з ВЧ-фокусуванням без урахування поля власного просторового заряду пучка; розглядається модель, що враховує некогерентні коливання частинок згустку, з використанням методу усереднення по швидким осциляціям. Отримані аналітичні результати перевіряються. Проводяться чисельні моделювання самоузгодженої динаміки низькоенергетичного іонного пучка.